Membrane and Water Treatment, *Vol. 14, No. 1 (2023) 47-54*
https://doi.org/10.12989/mwt.2023.14.1.047

Electrodialysis with a channeled stack for high strength cadmium removal from wastewater

Kyung Jin Min[1], Hyo Jin An[1], Ah Hyun Lee[1], Hyun-Gon Shin[2] and Ki Young Park[1*]

[1]*Department of Civil and Environmental Engineering, Konkuk University, 120 Neungdong-ro, Gwangjin-gu, Seoul 05029, Korea*
[2]*Department of Energy and Environmental Engineering, Shinhan University, Gyeonggi-do 480-857, Korea*

(Received September 29, 2022, Revised February 1, 2023, Accepted February 2, 2023)

Abstract. In this study, high concentrations of cadmium-containing wastewater were treated by electrodialysis (ED) with a channel stack. The limiting current density (LCD), cadmium removal efficiency, and current efficiency were investigated under each experimental condition according to the Reynolds number (Re), membrane area, and pH. With the increase in the film area to 111, 333, 555, and 777 cm^2 at Re (109.1), LCDs decreased to 408.11, 44.45, 35.32, and 13.64 A/m^2, respectively. The highest cadmium removal efficiency (99.6%) and current efficiency were obtained for the membrane area of 111 and 777 cm^2, respectively. Under changing Re in the pH range of 1 to 4, Re and LCD were proportional under the same pH condition, and pH and LCD tended to be inversely proportional under the same Re condition. Cadmium removal rate was the best at the pH range 3 - 4. It has been found that ED with channeled stacks can be successfully applied to treat wastewater containing high concentrations of cadmium.

Keywords: cadmium; channeled stack; electrodialysis; limiting current density; Reynolds number

1. Introduction

Zinc is not only an alloying element necessary for the plating of steel products, die-casting alloys, brass, etc., but is also a very important constituent material in primary batteries (Sohn 2019). However, the zinc smelting business environment is becoming increasingly difficult due to sluggish global economic growth, stringent environmental regulations, steady rise in energy costs, and the global supply chain crisis (Park *et al.* 2019, Yun 2015). The ores used in the zinc smelting process are mainly zinc blend, sphalerite, ZnS, etc., and sulfide ore is used as the main ore. In addition to zinc, raw ores contain copper, indium, iron, cadmium, silver, and sulfur dioxide, and are discharged as wastewater or residues, causing serious environmental pollution to the air, water, and soil and damaging biodiversity (Park *et al.* 2019).

In general, wastewater from zinc smelters contains high concentrations of heavy metals such as cadmium and is treated through traditional physicochemical treatments such as coagulation, sedimentation, and filtration (Yuan and Shi *et al.* 2009). These physicochemical treatment processes require large areas and use many chemicals as flocculants, and heavy metals discharged as sludge cannot be recovered (Benvenuti *et al.* 2014, Min *et al.* 2019). In contrast, membrane separation-based wastewater treatment technology requires minimum site area and use of chemicals through facility integration. In addition, heavy metals can be recovered from wastewater treatment processes in conjunction with zinc production or evaporation/extraction processes (Kim *et al.* 2022, Min *et al.* 2021c, Purkayasthha *et al.* 2014, Walker *et al.* 2014).

Electrodialysis (ED) is a membrane separation technology that alternately arranges an anion exchange membrane (AEM) and a cation exchange membrane (CEM) and applies an electric current to separate a solution with both low (diluent) and high (concentrate) concentration of ions. It has the advantage of not needing chemicals and minimum land area requirements. However, ED requires a significant amount of energy. To effectively use an ED treatment system, methods that can maximize energy efficiency must be applied (Gurreri *et al.* 2014, Min *et al.* 2021a, Walker *et al.* 2014).

The ion separation efficiency in electrodialysis depends on the physicochemical properties of metal ions as well as the characteristics of the applied ion exchange membrane and operating conditions (Cararescu *et al.* 2012). Selective ion separation using an ion exchange membrane is affected by the ion selectivity and dependence inherent in the ion exchange membrane and the concentration of metal ions to be removed. The ion removal efficiency is affected by the electrical properties due to the composition ratio of ions according to the influent characteristics and the potential difference in addition to the hydraulic properties such as the apparent surface velocity. Therefore, to achieve the required quality of wastewater treated using ED, optimal operating factors must be determined (Min *et al.* 2019).

To improve the energy efficiency of ED, it is necessary to reduce local resistance to mass transfer. In ED, at any point along the direction of fluid flow, ions are transported through an electrochemical potential gradient, resulting in entropy generation that lowers energy efficiency. This can be improved through better selection of ion exchange

---

*Corresponding author, Ph.D., Professor,
E-mail: kypark@konkuk.ac.kr
[a] Ph.D.

http://www.techno-press.org/?journal=mwt&subpage=7

ISSN: 2005-8624 (Print), 2092-7037 (Online)

Table 1 Characteristics of synthetic wastewater for each experimental condition

	Zinc refinery wastewater	pH 1	pH 2	pH 3	pH 4
pH	3.3 ± 0.1	1.07 ± 0.1	1.9 ± 0.2	2.9 ± 0.2	4.1 ± 0.1
Conductivity (mS/cm)	5.92 ± 0.15	12.58 ± 0.89	8.20 ± 1.40	6.20 ± 1.00	5.30 ± 1.00
Cd^{2+}(mg/L)	85.0 ± 3.6	96.4 ± 4.3	89.6 ± 13.5	106.0 ± 4.7	111.2 ± 3.7

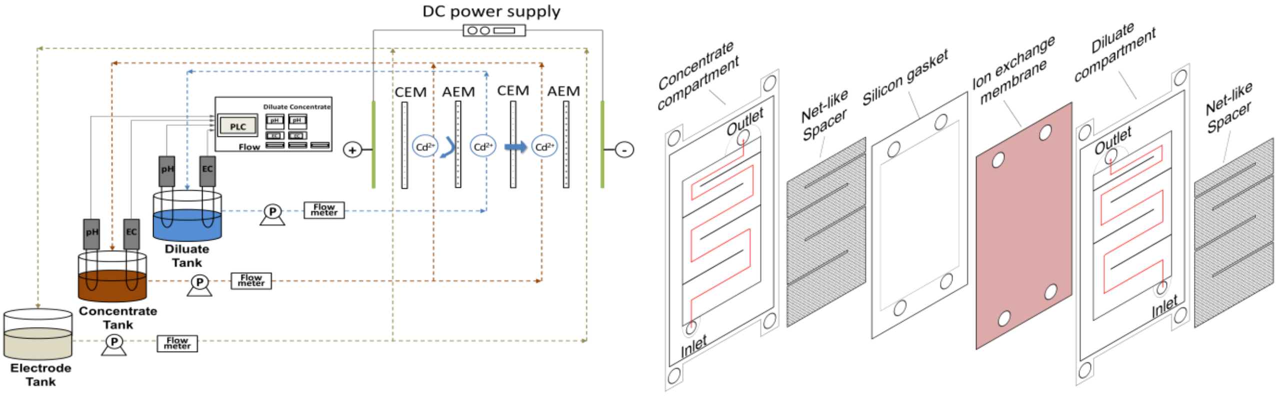

(a) Electrodialysis (b) Channel stack

Fig. 1 Schematic diagram of the experimental equipment

membranes and stack structures with thinner channels. Under the same flow rate conditions, the larger the system size, the larger the area of the ion exchange membrane, so it can be operated at lower current densities. Lower current densities reduce the energy required for mass transfer because the irreversibility due to the movement of ions decreases when the thermodynamic state is closer to equilibrium (Chehayeb *et al.* 2017, Min *et al.* 2022c).

The diffusion transport of ions is closely related to the membrane flow rate, however, because the membrane flow rate is proportional to the energy consumption, it has been operated while minimizing it. The stack geometry is fabricated to flow in one direction to avoid hydrostatic pressure differences as well as linear streamlines (Gurreri *et al.* 2012, Min *et al.* 2021b, Tedesco *et al.* 2012). However, if the stack is improved to have a serpentine path and the flow rate narrows down in the direction of the stack outlet such that the flow rate increases as it reaches the outlet, a faster flow rate can be provided at the same energy consumption. The ion removal efficiency can be improved by applying a higher voltage (or current) at a high flow rate (Min *et al.* 2021b).

Previous studies have focused on the effects of solution concentration and feed flow rates using brine or wastewater (Chao and Liang 2008, Daniilidis *et al.* 2014, Kingsbury *et al.* 2017, Tedesco *et al.* 2016, Tufa *et al.* 2014). However, the stacks used in various experiments have different geometries, making it difficult to support decisions regarding the optimal supply flow rate to ensure the maintenance costs and maximum current efficiency. ED performance evaluation according to the Reynolds number (Re) is one of the methods that can support economic decision making because it considers fluid properties such as system geometry, density, and viscosity (Ortiz-Martínez *et al.* 2020).

The purpose of this study was to derive the optimal operating factors using ED with a channeled stack to efficiently remove cadmium from zinc smelter wastewater. For this purpose, (a) the limiting current density (LCD), cadmium removal efficiency, and energy efficiency with respect to film area were investigated, and (b) the cadmium removal efficiency with respect to pH and Re was studied.

2. Materials and methods

2.1 Wastewater

Synthetic wastewater was prepared and tested to treat wastewater from a zinc smelter containing cadmium. The concentration of cadmium in the zinc smelter wastewater was 78.8 - 92.6 mg/L (85.0 mg/L), the electrical conductivity was 5.45 - 7.20 mS/cm (5.92 mS/cm), and the pH was 3.00 - 3.38 (3.31). Table 1 lists the properties of the synthetic wastewater prepared under each set of experimental conditions. Cadmium sulfate hydrate ($3CdSO_4\cdot 8H_20$, 98.0%, Samchun Pure Chemical Co., Ltd., Korea) was used as the cadmium source. HCl (1 N, Samchun Pure Chemical Co., Ltd., Korea) was used for the pH adjustment.

2.2 Electrodialysis setup

The The ED equipment used in this experiment was a diluate tank, concentrate tank, electrode rinse tank made of PVC, supply pumps, flow meters, pH/EC meters, power supplies, and data acquisition devices, as shown in Fig. 1 (a).

The capacity of each tank of the ED device was 0.5 L, the maximum supply flow rate of the circulation pump (P-F257H-SCV-96, Yusung Pumptech, Korea) was 43 L/min, and the power supply unit (EX50-36, ODA

Table 2 Main properties of the ion exchange membrane

Type	Cationic (Neosepta CMX)	Anionic (Neosepta AMX)
Thickness (mm)	0.17	0.14
Burst strength (MPa)	≥ 40	≥ 25
Electric resistance (Ω cm^2)	3.0	2.4
Ion exchange capacity (meq/g)	1.5 – 1.8	1.4 – 1.7

Technologies, Korea) could supply a maximum voltage of 50 V and a maximum current of 36 A. Samsan K.com-96pH (Samsankorea, Ltd., Korea) was used as the pH meter. SUNTEX EX-410 (Sechang Instruments, Korea) and FC-110 (Flos Korea, Korea) were used for electrical conductivity and flow meter, respectively.

All stacks of dilution and concentration cells were channeled with net-like spacers installed to induce zigzag flow to provide better turbulent flow and reduce concentration polarization (Fig. 1 (b)). The size of the stack used in this experiment was 115 mm (W) × 225 mm (H), the effective area of the ion exchange membrane was 48.5 cm2, and the total length of the channel was 33.9 cm. The size of the electrodes installed at both ends of the stack was 40 mm (W) × 90 mm (H) × 2 mm (D), and they were made of a titanium base plated with ruthenium (Ru) and iridium (Ir) to prevent corrosion.

2.3 Electrodialysis setup

Membrane processes such as ED are intrinsically affected by concentration polarization, resulting in a reduced driving force and consequent loss of efficiency. One way to counteract the negative effects of polarization is to use a mixing promoter, which generally acts as a spacer to maintain a fixed distance between the opposing membranes. Many studies have been conducted on the characterization of spacer-filled channels, most of which relate to the effect of spacer geometry on hydrodynamic function (Al-Sharif *et al.* 2013, La Cerva *et al.* 2017, Shakaib *et al.* 2012).

In this study, a common overlapping spacer shape formed by stacking two arrays of cylindrical rods was used. Among the Neosepta products of ASTOM (Tokyo, Japan) classified as homogeneous membranes, the ion exchange membrane used CMX for the cation exchange membrane and AMX for the anion exchange membrane (Table 2).

2.4 Operation conditions

The experiment was conducted in two steps: in the first step, to examine the effect of the ion exchange membrane area on the separation of cadmium, synthetic wastewater with a cadmium concentration of 110 mg/L was prepared and tested using a cadmium sulfate hydrate reagent. In the second step, the cadmium treatment efficiency was studied with the change in Re while changing the pH from 1 to 4. In all the experiments, the volumes of the diluent, concentrate, and electrode solution were set to 500 mL. As the electrolyte solution, 4% (w/w) Na_2SO_4 was used (Ji *et al.* 2017).

The LCD according to the film area was calculated at the same Re, and the cadmium removal efficiency and energy efficiency were investigated. While the Re of the diluent and concentrate was maintained at 109.1, the area of the ion exchange membrane was changed to 111, 333, 555, and 777 cm^2. In addition, the voltage was increased from 4 V to 40 V by 2 V, and after stabilizing for 2 min, the current was measured, and the LCD was calculated using the correlation between current (A) and current density (A/m^2). After obtaining the LCD in each experiment, it was operated using a constant voltage method for 30 min to investigate the cadmium treatment efficiency over time.

In order to examine the separation performance of cadmium with change in pH and Re, the pH was changed to 1, 2, 3, and 4, and ED was operated with Re 68.2, 81.8, 95.9, 109.1, 122.7, and 136.4, respectively. The total effective area of the cation and anion exchange membranes was 555 cm^2, and all experiments were repeated.

The ion exchange membrane used in the experiment was used after being immersed in the solution used for the experiment at 25 ± 1^{o}C for 24 h. At the end of the experiment, the ion exchange membrane was immersed in a solution containing 0.36% H_2SO_4 and 1.22% Na_2SO_4 (Sigma-Aldrich, Merck KGaA, Germany) for 1 h to remove the precipitate.

2.5 Analytical methods

In all experiments, electrical conductivity and pH were measured at 1-minute intervals using instruments installed in the dilution and concentration tanks. The resistance was calculated after measuring the voltage and current at 1-minute intervals. Initial concentrations of the diluted and concentrated sample solutions were measured prior to experiment. After the start of the test, the diluents and concentrates were collected every 5 min. The cadmium concentration in filtered (0.45 μm syringe filter) sample was measured at 226.5 nm wavelength using inductively coupled plasma optical emission spectroscopy (ICP-OES, ICP-6000, Thermo Fisher Scientific Inc., USA) according to the EN ISO 11885:2007 method.

Several definitions of Re can be found in the literature, depending on the choice of length and velocity scales (Al-Sharif *et al.* 2013, La Cerva *et al.* 2017, Koutsou *et al.* 2015, Saeed *et al.* 2015, Shakaib *et al.* 2012). The length scale can be assumed to be the filament diameter, channel height, or hydraulic diameter, or it can be assumed that the hydraulic diameter of the channel is equal to twice the channel thickness (Gurreri *et al.* 2016). Re was calculated using Eq. 1 (Bucs *et al.* 2015, Cipolliona *et al.* 2011, Mojab *et al.* 2014, Saeed *et al.* 2015, Shakaib *et al.* 2012).

$$Re = \frac{U_m d_h}{v} \tag{1}$$

where, U_m is the volume-averaged velocity along the main flow direction (m/s), d_h is the equivalent hydraulic diameter of channel (m), and v is the kinematic viscosity (m^2/s) of the fluid. In a spacer with overlapping filaments with distance i between the filaments and channel height H, dh can be calculated using Eq. 2 (Gurreri *et al.* 2016).

$$d_h = 2H\varepsilon \frac{l/H}{l/H + \pi/2} \tag{2}$$

where, l is the distance between the filaments (m), H is the height of the channel (m), and ε is the porosity. ε was calculated using Eq. 3 (Gurreri *et al.* 2016).

$$\varepsilon = \frac{l/H - \pi/8}{l/H} \tag{3}$$

In ED, the metal removal efficiency in the diluate was calculated using Eq. 4 (Ai *et al.* 2014).

$$Removal\ efficiency(\%) = 100\left[1 - \frac{[Cd]_t}{[Cd]_o}\right] \tag{4}$$

where, Cd_0 is the initial concentration of metal ions before the experiment (mg/L) and Cd_t is the concentration of metal ions at the elapsed time of each experiment (mg/L).

Although each stack consists of 5 pairs, since the charge passes through every pair of cells connected in series, the current efficiency can be expressed as (Min *et al.* 2021b) (Eq. 5):

$$\zeta = \frac{zFQC_s^{\Delta}}{IN} \tag{5}$$

where, ζ is the current efficiency, I is the total current (A) applied to the stack, C_s^{Δ} is the concentration (mol) difference between the feed and product solutions, z is the valence number of the ion, F is the Faraday constant (C/mol), Q is the volumetric flow rate (m^3/s), and N is the total number of cell pairs.

3. Results and discussion

3.1 LCD by ion exchange membrane area

The LCD is the most important factor affecting ED efficiency. However, it is difficult to determine the LCD because it varies depending on the channel structure of the stack and shape of the spacer (La Cerva *et al.* 2018, Mengual *et al.* 2014). LCD can be calculated using the current-voltage (V-I) curve or the current-current density. In this study, it was calculated using the current-current density (Min *et al.* 2021c).

The correlation between the ion exchange membrane area and the LCD was investigated at the same influent concentration. Because the LCD is a current at which the ion concentration on the surface of the ion exchange membrane becomes zero, the ion depletion increases as the electrolyte concentration in the bulk layer increases. Therefore, it could be seen using the LCD that the slope of the electric potential and the current changed due to the dissociation of water on the surface of the ion exchange membrane. As the area of the ion exchange membrane increased to 111, 333, 555, and 777 cm^2, the LCD decreased to 408.11, 44.45, 35.32, and 13.64 A/m^2, respectively, indicating that the areas of the ion exchange membrane and LCD tended to be inversely proportional. This is because electrical resistance increased as the spacer increased due to the increase in the number of ion exchange membranes. However, since the spacer partially blocked the current but increased the local current density, it could contribute to efficient heavy metal treatment even with a high film area.

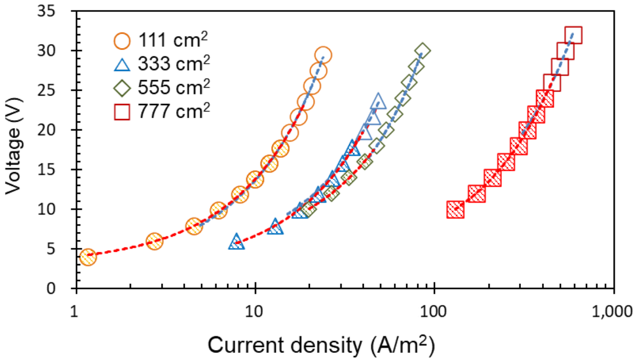

Fig. 2 Experimental LCD with respect to ion exchange membrane area

3.2 Cadmium removal and current efficiency by ion exchange membrane area

The highest electrical conductivity removal efficiency was obtained at the area of 111 cm^2 of the ion exchange membrane with the highest LCD. Removal efficiency of electrical conductivity in the area of 555 cm^2 was slightly better than that of 333 cm^2, and it was the lowest at the largest ion exchange membrane area of 777 cm^2 (Fig. 3).

As the rate of ion transfer through the ion exchange membrane increases with increase in applied voltage, the removal rate of ions in the initial stage was fast. However, the removal rate at 333 cm^2 area was relatively lower than that at 555 cm^2, which may be due to concentration polarization caused by the high applied voltage and the small effective area. In the 333 cm^2 area, water splitting can begin quickly because of the high relative ion removal rate at the beginning of the operation. When the water splitting rate is higher in CEM than in AEM, the formation of divalent cation hydroxide, a scale material, is promoted on the surface of CEM. H^+ generated by water splitting reduces the surface charge of the precipitate, which can lead to the accumulation of scale material and thus intensify fouling (Andreeva *et al.* 2018). Therefore, when concentration polarization occurs in a small area, fouling is promoted, but if the ion exchange membrane area is small, the effective area is greatly reduced, so the removal efficiency can be rapidly reduced. Therefore, the generation of fouling in the

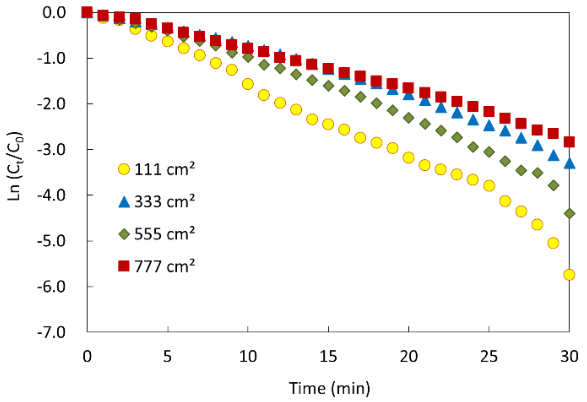

Fig. 3 Removal of electrical conductivity with respect to the area of ion exchange membrane

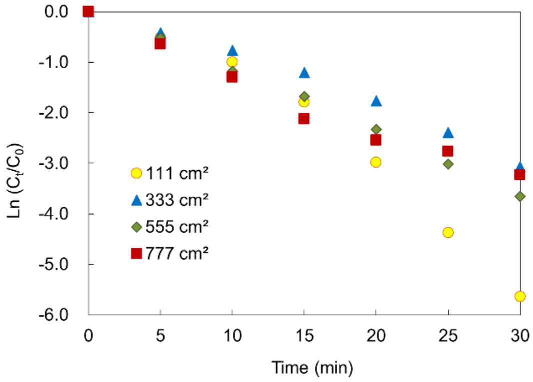

Fig. 4 Cadmium removal with respect to the area of the ion exchange membrane

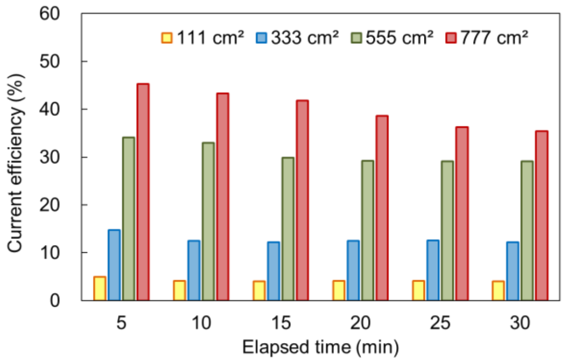

Fig 5. Current efficiency with respect to the area of ion exchange membrane

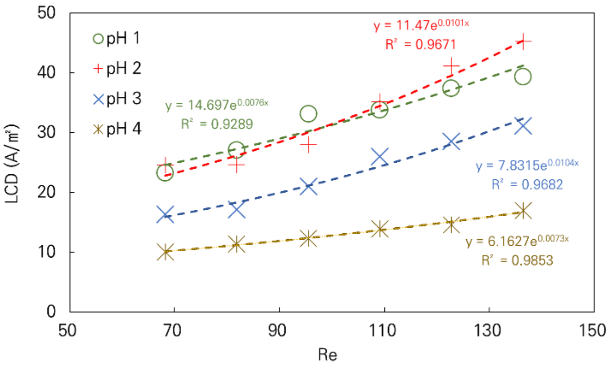

Fig. 6 Correlation between Re and LCD by pH

333 cm^2 area may be the cause of the reduction in the removal rate. Since the total amount of scale material generated is the same, this phenomenon will not appear if the membrane area is increased.

The trend of cadmium removal efficiency was similar to that of the electrical conductivity. It was the highest at the ion exchange membrane area of 111 cm^2, followed by that at 555 cm^2. The cadmium removal efficiency at the ion exchange membrane area of 777 cm^2 was slightly higher that that at 333 cm^2, but the difference was not significant (Fig. 4). This result is different from that of a previous study, in which the area of the ion exchange membrane and the treatment efficiency were proportional (Min. *et al.* 2021c). This is because this difference can be affected by the selectivity of the ion exchange membrane, membrane movement such as water transport by osmosis and electroosmosis, leakage current, and contamination (Lee 2011). In particular, considering that the selectivity of the ion exchange membrane largely depends on the salt concentration of the external solution, this can be attributed to the difference in the influent.

In all experiments, when the concentration of cadmium was reduced to 10 mg/L or less, the removal efficiency dropped sharply, therefore, it is reasonable from an economic point of view to treat it to an appropriate level. The total cost of ED is the sum of the initial investment, energy, and maintenance costs. The initial investment cost was proportional to the area of the ion exchange membrane, and the energy cost was linearly proportional to the current density. However, the energy and investment costs are inversely proportional. Therefore, to optimize the total cost, it is necessary to determine the optimal current density. The optimal current density was determined by measuring the current efficiency under various experimental conditions. In the ion exchange membrane areas of 555 cm^2 and 777 cm^2, the current efficiency gradually decreased as the operating time elapsed. After 30 min, the current efficiencies were 35.4% at 777 cm^2 and 29.2% at 555 cm^2 (Fig. 5). On the other hand, very low current efficiencies were maintained at 111 cm^2 (< 5%) and 333 cm^2 (< 14.7%) of the ion exchange membrane area, regardless of the operating duration. In ED, the concentration of the diluate and the diffusion flux are proportional, therefore, when the operating time is increased, the diffusion flux decreases as the concentration of the diluent and the current efficiency decreases (Bernardes *et al.* 2016). When the concentration of the diluent decreases owing to a decrease in the number of pairs of ion exchange membranes, the current efficiency may decrease rapidly owing to the high applied voltage. Considering the current efficiency, an ion exchange membrane area of 777 cm^2 was found to be the most suitable, but considering the cadmium removal efficiency, a membrane area of 555 cm^2 was the most suitable.

3.3 Limiting current density (LCD) by Re and pH

Changes in the Re and pressure of a solution cause significant differences in the solute permeation through the ion exchange membrane. The effect of Re on the LCD depends on the salt concentration, which is related to the

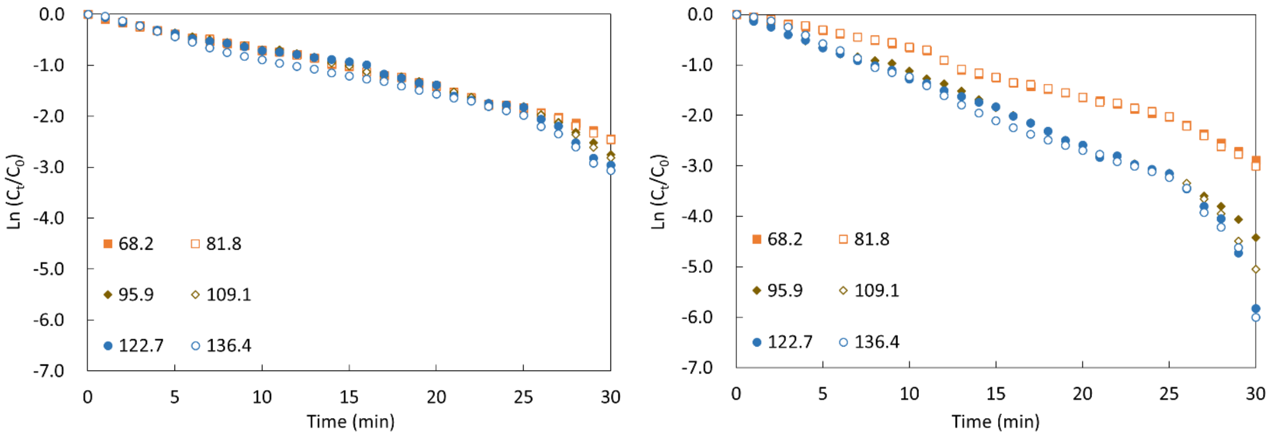

(a) pH 1 (b) pH 2

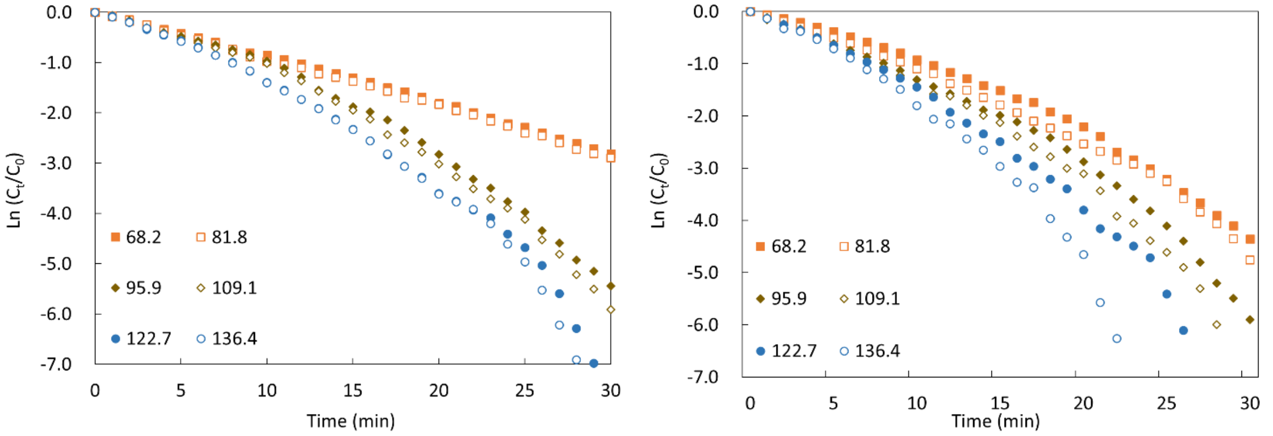

(c) pH 3 (d) pH 4

Fig. 7 Change in electrical conductivity with respect to Re and pH

boundary layer thickness. In solutions with high salt concentrations, the relative importance of the diffusion boundary layer owing to Re is limited.

However, as the concentration decreased, the relative importance of the diffusion boundary layer increased because the mixing intensity increases with an increase in Re. Using an ion exchange membrane of area of 555 cm^2, the pH and Re were changed to obtain an LCD. The experiment showed that the LCD was high at pH 1 when the Re was low, but LCD was highest at pH 2 when the Re exceeded 100. The LCD at pH 3 was higher than that at pH 4 at the same Re, which was consistent with the hydrogen ion concentration at a lower pH (Fig. 6). This phenomenon appears to be due to the cadmium concentration of the initial dilution water. The cadmium concentration of the initial dilution water at pH 2 was the lowest in all conditions and was more than 7% lower than that at pH 1. The relative importance of the diffusion boundary layer increases as the concentration decreases because the mixing strength increases as Re increases. Therefore, this is a result confirming the relative importance of the diffusion boundary layer for the concentration.

3.4 Cadmium removal

The electrical conductivity and cadmium removal efficiency were investigated with respect to the operating time under each pH condition (Fig. 7). The removal efficiency of electrical conductivity was slowest at pH 1 and fastest at pH 4. In addition, the electrical conductivity removal rate at pH 3 was higher than that at pH 2. This difference may be due to the difference in initial electrical conductivity. Under the applied pH conditions, Re and electrical conductivity removal efficiency showed a proportional relationship.

The Reynolds number and cadmium removal efficiency exhibited a directly proportional correlation under all conditions, similar to the electrical conductivity results. This is contrary to the results of the study that cadmium exists as ions in a solution with a pH < 7, so it can be removed through ED, however, there is no difference in the cadmium removal rate with change in pH under the same flow rate condition of pH 7 or less (Ali *et al.* 2014). Fig. 8 shows the cadmium removal efficiency with Re at pH 1 - 4, similar to the initial pH of cadmium wastewater. Cadmium removal rate on Re shows almost similar trend for pH 2 - 4 but pH 1 seemed to be distracted as compared to the other cases. pH 2 - 4 showed an exponential growth and reached at a plateau (limit) with increase of Re, but pH 1 stayed almost same and increased slightly. This difference appears to be due to the cadmium concentration of the initial dilute. As mentioned above, this shows that the concentration of cadmium in the initial diluted solution was significantly affected by the diffusion boundary layer because it was the

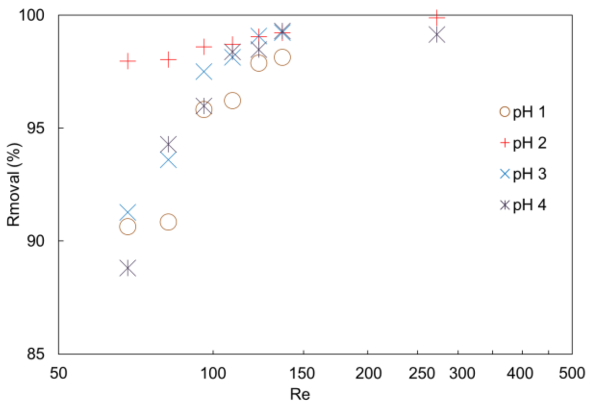

Fig. 8 Cadmium Removal by Re

lowest in all conditions at pH 2. When Re increased under the same pH conditions, the cadmium removal efficiency also increased, but there was no significant difference under Re 100 or higher. An increase in Re increased the velocity perpendicular to the main flow direction in the ion exchange membrane, resulting in better mixing. However, there is a limit to the increase in Re owing to the flow rate that can be supplied because the channels are thin and there are restrictions to the shape, such as the spacing and thickness of the spacer. This result is consistent with that of a report that the porosity of the spacer can be maximized when it is larger than a Re of 90 in a general overlapping spacer shape formed by stacking cylindrical rods in two rows (Gurreri *et al.* 2016).

4. Conclusions

In this study, ED was used to remove cadmium from wastewater generated from a Zn smelter. A channeled stack, which has a tortuous path developed to increase LCD and prevent concentration polarization and narrows down in the direction of the outlet, was applied to the ED process. LCD, cadmium removal efficiency, and energy efficiency according to the ion exchange membrane area, and cadmium removal efficiency according to pH and Re were investigated. The increase in the area of the ion exchange membrane with respect to the increase in the ion exchange membrane pair showed an inverse correlation between the voltage and LCD, owing to the electrical resistance of the ion exchange membrane and the current blocked by the spacer. If the area of the ion exchange membrane is minimized and the applied voltage is increased, the operating time can be effectively shortened, however, the current efficiency is low, resulting in poor economic feasibility. In relation to the efficiency of the current, the current efficiency decreases as the processing efficiency increases, because ion transport depends on the supplied charge, according to Faraday's law. Voltage and LCD showed a correlation with Re, indicating that Re affected the thickness of the diffusion boundary layer on the surface of the ion exchange membrane, suggesting that Re is an important operating variable for low-salt solution treatment. When Re was increased under the same pH conditions, the removal efficiency of cadmium also increased, however, there was no significant difference under the condition of Re 100 or higher.

Acknowledgments

This paper was supported by Konkuk University Researcher Fund in 2022, and Waste to Energy-Recycling Human Resource Development Project (YL-WE-21-001).

References

Al-Sharif, S., Albeirutty, M., Cipollina, A. and Micale, G. (2013), "Modelling flow and heat transfer in spacer-filled membrane distillation channels using open source CFD code", *Desalination*, **311**, 103-112. https://doi.org/1016/j.desal.2012.11.005.

Ali, M. S., Hafiane, A., Dhahbi, M. and Hamrouni, B. (2014), "Electrodialytic removal of cadmium from brackish water: effects of operating parameters", *J. Memb. Sep. Technol.*, **3**(2), 67-77. https://doi.org/10.6000/1929-6037.2014.03.02.1.

Andreeva, M.A., Gil, V.V., Pismenskaya, N.D., Dammak, L., Kononenko, N.A., Larchet, C., Grande, D., Nikonenko, V.V. (2018), "Mitigation of membrane scaling in electrodialysis by electroconvection enhancement, pH adjustment and pulsed electric field application", *J. Membr. Sci.*, **549**, 129-140. https://doi.org/10.1016/j.memsci.2017.12.005.

Benvenuti, T., Krapf, R.S., Rodrigues, M.A.S., Bernardes, A.M. and Zoppas-Ferreira, J. (2014), "Recovery of nickel and water from nickel electroplating wastewater by electrodialysis", *Sep. Purif. Technol.*, **129**, 106-112. https://doi.org/10.1016/j.seppur.2014.04.002.

Cararescu, S., V. Purcar, and D. Vaireany. (2012), "Separation of copper ions from synthetically prepared electroplating wastewater at different operating conditions using electrodialysis", *Sepa. Sci. Technol.*, **47**(16), 2273-2280. https://doi.org/10.1080/01496395.2012.669444.

Chao, Y. M. and Liang, T.M. (2008), "A feasibility study of industrial wastewater recovery using electrodialysis reversal", *Desalination*, **221**(1-3), 433-439. https://doi.org/10.1016/j.desal.2007.04.065.

Chehayeb, K.M. and Lienhard, J.H. (2017), "Entropy generation analysis of electrodialysis", *Desalination*, **413**, 184-198. https://doi.org/10.1016/j.desal.2017.03.001.

Daniilidis, A., Vermaas, D.A., Herber, R. and Nijmeijer, K. (2014), "Experimentally obtainable energy from mixing river water, seawater or brines with reverse electrodialysis", *Renew. Energy*, **64**, 123-131. https://doi.org/10.1016/j.renene.2013.11.001.

Gurreri, L., Tamburini, A., Cipollina, A. and Micale, G. (2012), "CFD analysis of the fluid flow behavior in a reverse electrodialysis stack", *Desalin. Water Treat.*, **48**(1), 390-403. https://doi.org/10.1080/19443994.2012.705966.

Gurreri, L., Tamburini, A., Cipollina, A., Micale, G. and Ciofalo, M. (2014), "CFD prediction of concentration polarization phenomena in spacer-filled channels for reverse electrodialysis", *J. Membr. Sci.*, **468**, 133-148. https://doi.org/10.1016/j.memsci.2014.05.058.

Gurreri, L., Tamburini, A., Cipollina, A., Micale, G. and Ciofalo, M. (2016), "Flow and mass transfer in spacer-filled channels for reverse electrodialysis: a CFD parametrical study", *J. Membr. Sci.*, **497**, 300-317. https://doi.org/10.1016/j.memsci.2015.09.006.

Ji, Z.Y., Chen, Q.B., Yuan, J.S., Liu, J., Zhao, Y.Y. and Feng, W.X. (2017), "Preliminary study on recovering lithium from high Mg2+/Li+ratio brines by electrodialysis", *Sep. Purif. Technol.*, **172**, 168-177. https://doi.org/10.1016/j.seppur.2016.08.006.

Kim, J., Yoon, S., Choi, M., Min, K.J., Park, K.Y., Chon, K. and Bae, S. (2022), "Metal ion recovery from electrodialysis-concentrated plating wastewater via pilot-scale sequential electrowinning/chemical precipitation", *J. Clean. Prod.*, **330**, 129879. https://doi.org/10.1016/j.jclepro.2021.129879.

Kingsbury, R.S., Liu, F., Zhu, S., Boggs, C., Armstrong, M.D., Call, D.F. and Coronell, O. (2017), "Impact of natural organic matter and inorganic solutes on energy recovery from five real salinity gradients using reverse electrodialysis", *J. Membr. Sci.*, **541**, 621-632. https://doi.org/10.1016/j.memsci.2017.07.038.

La Cerva, M., Ciofalo, M., Gurreri, L., Tamburini, A., Cipollina, A. and Micale, G. (2017), "On some issues in the computational modelling of spacer-filled channels for membrane distillation", *Desalination*, **411**, 101-111. https://doi.org/10.1016/j.desal.2017.02.016.

La Cerva, M., Gurreri, L., Tedesco, M., Cipollina, A., Ciofalo, M., Tamburini, A. and Micale, G. (2018), "Determination of limiting current density and current efficiency in electrodialysis units", *Desalination*, **445**, 138-148. https://doi.org/10.1016/j.desal.2018.07.028.

Lee, G. (2011), "Effects of operating parameters on the removal performance of electrodialysis for treating wastewater containing cadmium", *Desalin. Water Treat.*, **35**(1-3), 150-157. http://dx.doi.org/10.5004/dwt.2011.2850.

Min, K.J., Choi, S.Y., Jang, D., Lee, J. and Park, K.Y. (2019), "Separation of metals from electroplating wastewater using electrodialysis", *Energ. Source Part A*, **41**(20), 2471-2480. https://doi.org/10.1080/15567036.2019.1568629.

Min, K.J., Kim, J.H. and Park, K.Y. (2021a), "Characteristics of heavy metal separation and determination of limiting current density in a pilot-scale electrodialysis process for plating wastewater treatment", *Sci. Total Environ.*, **757**, 143762. https://doi.org/10.1016/j.scitotenv.2020.143762.

Min, K.J., Kim, J.H., Kim, S.W., Lee, S., Shin, H.G., and Park, K.Y. (2021b), "Copper and nickel removal from plating wastewater in the electrodialysis process using a channeled stack", *Membr. Water Treat.*, **12**(4), 149-155. https://doi.org/10.12989/mwt.2021.12.4.149.

Min, K.J., Kim, J.H., Oh, E.J., Ryu, J.H. and Park, K.Y. (2021c), "Flow velocity and cell pair number effect on current efficiency in plating wastewater treatment through electrodialysis", *Environ. Eng. Res.*, **26**(2), 190502. https://doi.org/10.4491/eer.2019.502.

Ortiz-Martínez, V.M., Gómez-Coma, L., Tristán, C., Pérez, G., Fallanza, M., Ortiz, A. and Ortiz, I. (2020), "A comprehensive study on the effects of operation variables on reverse electrodialysis performance", *Desalination*, **482**, 114389. https://doi.org/10.1016/j.desal.2020.114389.

Park, H.S., Kim, T.Y. and Kim, D. (2019). "Efficiency analysis of zinc refining companies", *Sustain.*, **11**(22), 6528. https://doi.org/10.3390/su11226528.

Purkayasthha, D., Mishra, U. and Biswas. S. (2014), "A comprehensive review on Cd (II) removal from aqueous solution", *J. Water Proc. Eng.*, **2**, 105-128. https://doi.org/10.1016/j.jwpe.2014.05.009.

Saeed, A., Vuthaluru, R. and Vuthaluru, H.B. (2015), "Investigations into the effects of mass transport and flow dynamics of spacer filled membrane modules using CFD", *Chem. Eng. Res. Des.*, **93**, 79-99. https://doi.org/10.1016/j.cherd.2014.07.002.

Shakaib, M., Hasani, S.M.F., Ahmed, I. and Yunus, R.M. (2012), "A CFD study on the effect of spacer orientation on temperature polarization in membrane distillation modules", *Desalination*, **284**, 332-340. https://doi.org/10.1016/S0376-7388(01)00494-X.

Sohn, H. (2019), "Current Status of Zinc Smelting and Recycling", *J. Korean Inst. Resour. Recycl.*, **28**(5), 30-41. https://doi.org/4/kirr.2019.28.5.30.

Tedesco, M., Cipollina, A., Tamburini, A., van Baak, W. and Micale, G. (2012), "Modelling the Reverse ElectroDialysis process with seawater and concentrated brines", *Desalin. Water Treat.*, **49**(1), 404-424. https://doi.org/10.1080/19443994.2012.699355.

Tedesco, M., Scalici, C., Vaccari, D., Cipollina, A., Tamburini, A. and Micale, G. (2016), "Performance of the first reverse electrodialysis pilot plant for power production from saline waters and concentrated brines", *J. Membr. Sci.*, **500**, 33-45. https://doi.org/10.1016/j.memsci.2015.10.057.

Tufa, R.A., Curcio, E., van Baak, W., Veerman, J., Grasman, S., Fontananova, E. and Di Profio, G. (2014), "Potential of brackish water and brine for energy generation by salinity gradient power-reverse electrodialysis (SGP-RE)", *RSC Adv.*, **4**(80), 42617-42623. https://doi.org/10.1039/C4RA05968A.

Walker, W.S., Kim, Y. and Lawler, D.F. (2014), "Treatment of model inland brackish groundwater reverse osmosis concentrate with electrodialysis-Part I: Sensitivity to superficial velocity", *Desalination*, **344**, 152-162. https://doi.org/10.1016/j.desal.2014.03.035.

Yuan, Z. and Shi, L. (2009), "Improving enterprise competitive advantage with industrial symbiosis: case study of a smeltery in China", *J. Clean. Prod*, **17**(14), 1295-1302. https://doi.org/10.1016/j.jclepro.2009.03.016.

Yun, J.J. (2015), "How do we conquer the growth limits of capitalism? Schumpeterian dynamics of open innovation", *J. Open Innov.*, **1**(2), 17. https://doi.org/10.1186/s40852-015-0019-3.

SP